Defence Science Journal, Vol. 58, No. 1, January 2008, pp. 34-45

Finite Element Analysis of Collapse of Metallic Tubes

P.K. Gupta[1], N.K. Gupta[2] and G.S. Sekhon [2]

[1]*Indian Institute of Technology, Roorkee–247 667*
[2]*Indian Institute of Technology Delhi, New Delhi–110 016*

ABSTRACT

Quasi-static axial and lateral compression tests were conducted on aluminium tubes of circular, rectangular, and square cross sections on a universal testing machine (Instron model 1197). During the compression process, different tubes were collapsed in different modes of collapse. These compression processes were also modelled using FORGE2 finite element code. The code has the capabilities of automatic mesh generation, modelling of die, creation of material data file, carrying out the finite element computations, and post-processing of results. The deforming tube material was modelled as rigid-visco-plastic. Development of different modes of collapse was investigated experimentally and computationally. The experimental load-compression curves and deformed shapes are compared with the computed results and found in good agreement. It is found that the proposed finite element models of the different compression processes are capable of predicting the modes of collapse.

Keywords: Metallic tubes, quasi-static loading, mode of deformation, FORGE2, energy-absorbing devices

NOMENCLATURE

$\dot{\bar{\varepsilon}}$	Effective strain rate
$\bar{\varepsilon}$	Effective strain
β	Temperature sensitivity term
T	Temperature in absolute value
τ	Shearing stress
Ω	Contact surface between platen and tube
D	Mean diameter of tube
t	Thickness of tube
S_f	Frictional surface
α	Coefficient of friction
Δv	Relative sliding velocity between platen and tube

1. INTRODUCTION

Metallic tubes that absorb the kinetic energy by undergoing plastic deformation are found to be efficient as energy-absorbing devices. Plastic collapse of thin-walled shells of various shapes, sizes, and materials under different loading conditions has been studied in the past[1-5]. The important characteristics of the impact energy absorbers, their selection criteria, and various modes of plastic deformation of thin-walled shells such as flattening, splitting, tube inversion and folding, have been discussed in detail[6]. Johnson and Reid[7] reviewed the modes of deformation of various thin-walled shells and their corresponding load-compression graphs. The exact behaviour of the tubes is a very complex process due to its dependency upon many process parameters.

Received 20 January 2006, revised 25 November 2006

Some of the process parameters are diameter-to-thickness ratio, length-to-thickness ratio, and friction between the platen-tube interfaces. Therefore, the prediction of deforming behaviour is difficult. The compression process of metallic tubes of different shapes and sizes under different loading and different support conditions were investigated by many researchers in the past few decades by considering different analytical models of collapse[8-25]. Recently, finite element codes have also been employed to understand the compression process by few researchers[26-28].

Since finite element method has reached a state of maturity, numerical simulation can be carried out as an alternative to the experiments to understand the basic compression process involved in the collapse of metallic shells. Therefore, in this paper, an attempt has been made to understand the axial and lateral compression of aluminium shells between the two parallel rigid plates under quasi-static loading with finite element simulations. But to develop and validate the computational finite element models, experiments were also performed and the results are compared with the computations. This paper presents experimental and computational studies of the energy-absorbing characteristics of the metallic tubes having circular, square, and rectangular cross sections madeup of aluminium. These tubes were subjected to axial and lateral compression tests. Finite element code FORGE2[29] has been used to simulate the compression processes. The results, thus, obtained are analysed, compared and discussed. On the basis of the different proposed computational models, the collapse behaviour of the tubes is predicted.

2. EXPERIMENTAL WORK

In the experiments, test specimens were compressed under quasi-static loading using a universal testing machine (Instron model 1197) of 50 T capacity. The load versus cross-head movement plots were obtained from the automatic chart recorder of the machine. To study the history of deformation, deformed shapes at different stages of compression were recorded. The following three series of experimental investigations were carried out:

2.1 Axial Compression of Round-hollow-thin and Thick-walled Aluminium Tubes

The test specimens were placed on the bottom platen of the machine with their axis aligned vertically. During the loading process, the top platen was moved downward at a speed of 10 mm/min. The length of the test specimens was taken as twice of their outer diameter. The diameter-to-wall thickness ratio (*D/t)* was varied from 7.23 to 37.46. Table 1(a) gives dimensions of the test specimens used during the experiments. The tubes were tested in the as-received conditions. It was found that all the tubes with *D/t* ratio between 10 and 23 deformed in axisymmetric concertina mode of collapse, while the tube specimen having *D/t* ratio of 7.23 deformed in axisymmetric multiple-barrelling mode of collapse [Figs 1(a) and 1(b)].

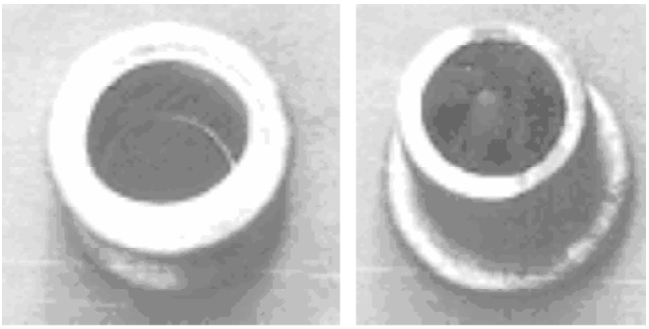

(a) (b)

Figure 1[(a)-(b)]. True modes of collapse of different tubes subjected to different loadings: (a) axisymmetric multiple barrelling of round tube subjected to axial load and (b) axisymmetric concertina mode of collapse of round tube subjected to axial load.

2.2 Lateral Compression of Hollow Tubes of Circular Cross Section under Quasi-static Loading

Aluminium tubes were tested after annealing. Annealing of the tubes was done by soaking the test specimens at 360 °C for 30 min in a furnace and allowing them to cool gradually for 24 h. The tubular specimens were kept between the two rigid platens with their axes aligned horizontally. Each test specimen was placed on the bottom platen and the top platen was moved at a speed of 10 mm/min. The length of each specimen was 100 mm. Other pertinent dimensions of the test

Table 1(a). Dimensions of specimens used for compression of round tubes

Specimen	Average diameter (D) (mm)	Thickness (t) (mm)	D/t	Material properties					
				Axial compression			Lateral compression		
				K_0 (MPa)	a	m	K_0 (MPa)	a	m
AC253	21.93	3.03	7.23	140.50	1.122	0.0013	159.7	1.450	0.0251
AC252	23.06	2.04	11.30	136.20	1.758	0.0120	140.3	1.416	0.0819
AC251	24.27	1.03	23.56	111.30	2.380	0.0015	159.7	1.240	0.0251
AC383	34.73	3.13	11.09	142.20	1.340	0.1260	161.3	1.650	0.0271
AC381	36.93	1.03	35.85	134.80	2.800	0.0012	159.4	1.453	0.0259
AC503	47.66	3.44	13.85	138.50	1.910	0.0034	153.3	1.451	0.0244
AC502	48.92	1.68	29.12	143.50	1.915	0.0002	145.1	1.452	0.0280
AC501	48.70	1.30	37.46	146.20	1.910	0.0001	161.3	1.652	0.0272
AC802	79.20	2.18	36.33	89.36	0.610	0.0001	125.2	1.250	0.0215

test specimens are given in Table 1(a). It was found that all the specimens deformed in a single mode of collapse [Fig. 1(c)].

2.3 Lateral Compression of Square and Rectangular Tubes under Quasi-static Loading

Annealed aluminium tubes were subjected to lateral compression. The test specimens were placed laterally on the bottom platen and the load was applied by moving the top platen at a downward speed of 10 mm/min. The length of each test specimen was 100 mm. Cross-sectional dimensions of the specimens used in the study are given in Table 1(b). It was found that all the specimens deformed in a single mode of collapse [Fig. 1(d)].

For circular cross-sectional tubes, the diameter-to-thickness *(D/t)* ratio has been varied to see its effect on the energy-absorbing capacity of tubes. The *D/t* ratio was varied from 7.23 to 37.46. For the same diameter, thickness of the tubes was varied and vice versa, so that the effect of thickness variations for the same diameter tubes and the effect of diameter variations for the same thickness can be investigated. The cross-sectional dimensions of rectangular and square sections were also varied. In some cases of rectangular tubes, for the same cross-sectional dimensions, the thickness was varied. Some series of experiments were performed in as-received conditions of tube specimens, while others after annealing the tubes. The different modes of deformation of tubes under different loading conditions are shown in Fig. 1[(a)-(d)].

3. ANALYSIS

The compression processes have been modelled and the different modes of deformation of the tubes during the compression process have been analysed using the finite element method. The details of the formulation are provided[26]. The material of the tubes is assumed as homogeneous, isotropic, incompressible, and rigid-visco-plastic. The constitutive

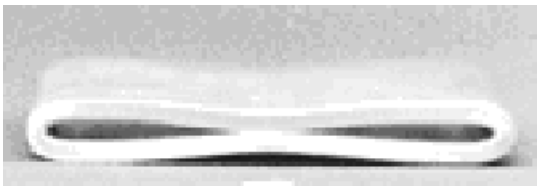

(c)

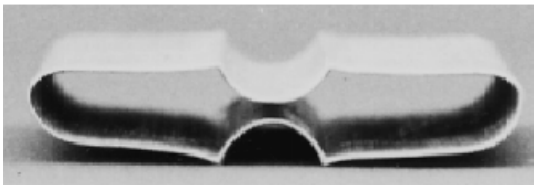

(d)

Figure 1[(c)-(d)]. True modes of collapse of different tubes subjected to different loadings: (c) flattening of round tube subjected to lateral load and (d) flattening of rectangular and square tubes subjected to lateral load.

relation for such a material is given by the Norton-Hoff law[30] as

$$S = 2K(\sqrt{3}\bar{\dot{\varepsilon}})^{m-1}\dot{\varepsilon}_{ij} \quad (1)$$

where $\dot{\varepsilon}_{ij} = \frac{1}{2}(V_{i,j} + V_{j,i})$ and S is the components of the deviatoric stress tensor and $\dot{\varepsilon}$ is the corresponding components of the strain tensor. The incompressibility condition is:

$$div(V) = 0 \ on \ \Omega \quad (2)$$

The material consistency K, which is a function of strain and temperature, is given by

$$K = K_0(1 + a\bar{\varepsilon})e^{\beta/T} \quad (3)$$

where K_0, a and β are the material constants. Consequently, the constitutive law assumes the form:

$$\bar{\sigma} = K_0(1 + a\bar{\varepsilon})\bar{\dot{\varepsilon}}^m \quad (4)$$

The friction between the tube and the tool is platen with a visco-plastic law[30]:

$$\tau = \alpha K|\Delta V|^{p-1}\Delta V \ \text{ on } S_f \quad (5)$$

where α is the coefficient of friction, ΔV is the relative sliding velocity between the platen and the tube, p is a constant and S_f denotes the frictional surface. The material parameters strain rate sensitivity index (m), strain-hardening parameter (a) and a constant (K_0) were calculated by conducting uniaxial tension tests on standard specimens at the three different strain-rates. Figure 2 shows the true stress versus true strain graphs after annealing of specimen AC503 at the three different strain rates to find the material parameters. These material parameters for different tube specimens are presented in Table 1. The value of p was taken equal to the value of strain rate sensitivity index (m).

The compression process of round and rectangular tubes under lateral load is a case of plane strain, while of round tube under axial load is a case of axisymmetric deformation. The finite element models

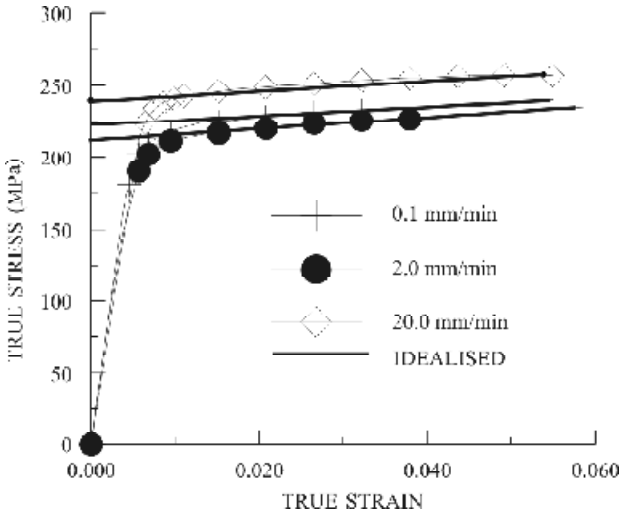

Figure 2. Typical true stress and true strain graph of uniaxial tension test for specimen AC503 used for lateral compression.

of different compression processes of the tubes along with the moving die and its boundary conditions before the compression are shown in Figure 3[(a-d(1)]. Figure 3[(a-d(2)] shows the typical computed modes of deformation of the tubes in different compression processes. The six-noded triangular elements have been used to descretise the domain. The temperature is kept constant and equal to room temperature (310K) during the entire process of compression. The contact between the die and the workpiece has been assumed as unilateral. The increment in each step of deformation is taken as 1 per cent of an average strain.

Comparison of typical experimental and computational load-compression and energy-compression curves in different compression processes are shown in Figs 4 and 5. The energy-compression curve was obtained by integrating the corresponding load-compression curve. It is clear from these figures that the two sets are found to be in good agreement.

3.1 Variation of Predicted Contours of Equivalent Strain

The contours of equivalent strain for different compression processes at the two typical stages have been presented in Fig. 6 to understand the collapse processes of the various tubes under consideration.

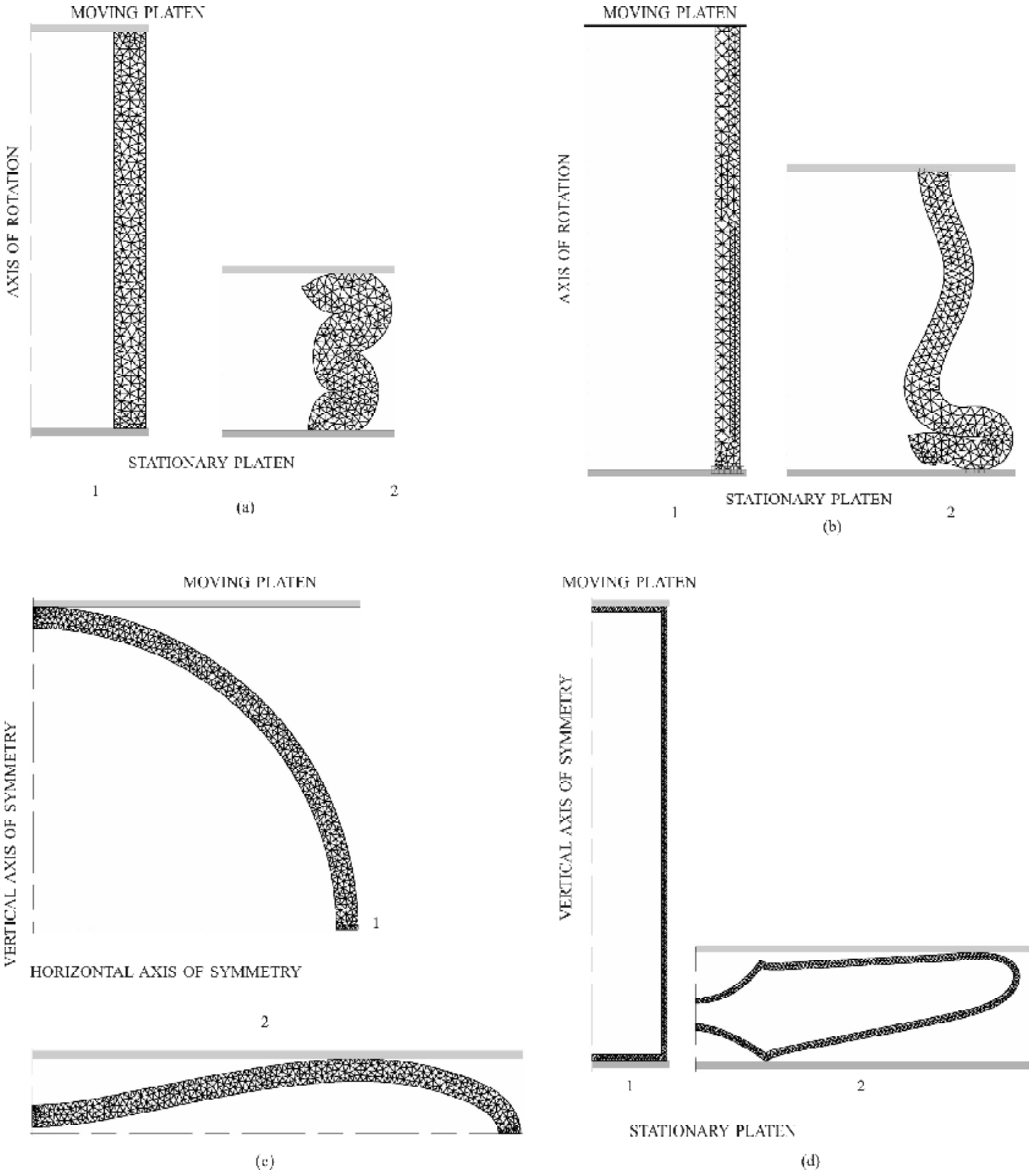

Figure 3. Computed modes of collapse of different tubes subjected to different loadings: (1) before compression, (2) after compression; (a-2) axisymmetric multiple barrelling of round tube subjected to axial load; (b-2) axisymmetric concertina mode of collapse of round tube subjected to axial load; (c-2) flattening of round tube subjected to lateral load, and (d-2) flattening of rectangular and square tubes subjected to lateral load.

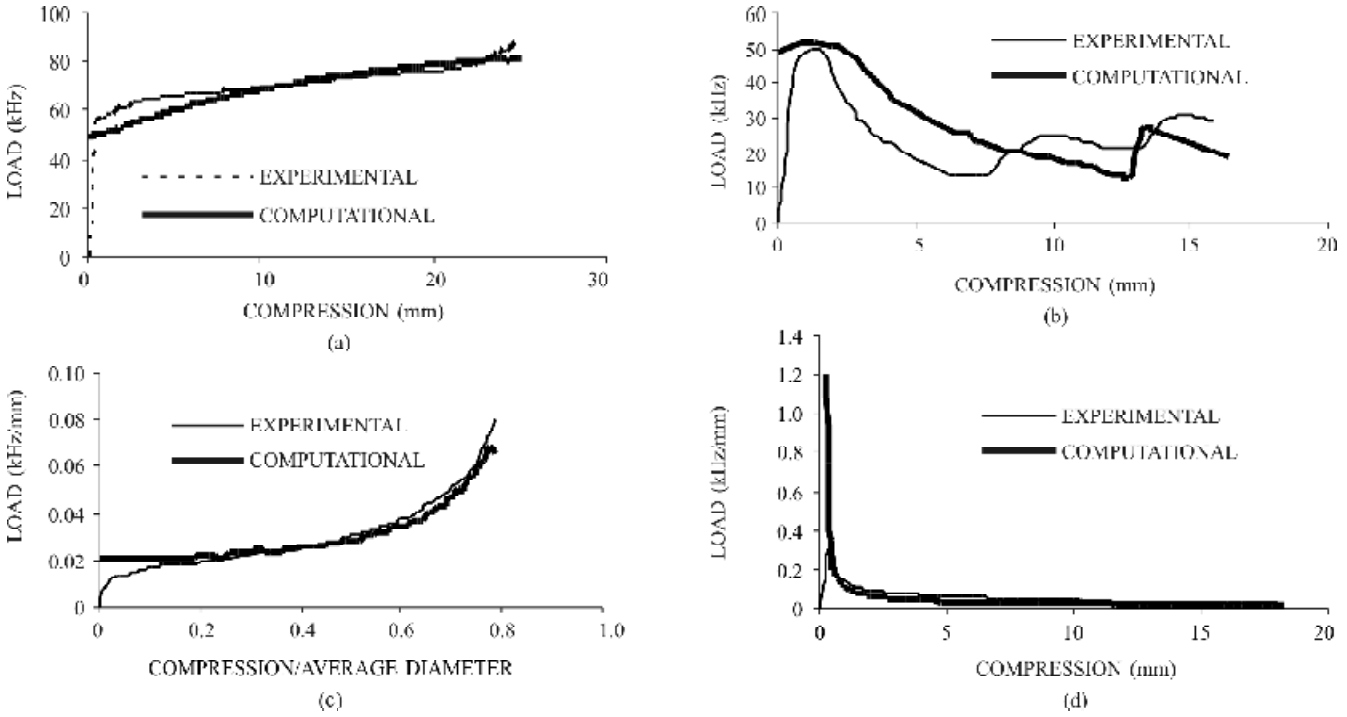

Figure 4. Comparison of experimental and computed load-compression curves: (a) axisymmetric multiple barrelling of round tube subjected to axial load, (b) axisymmetric concertina mode of collapse of round tube subjected to axial load, (c) flattening of round tube subjected to lateral load, and (d) flattening of rectangular and square tubes subjected to lateral load.

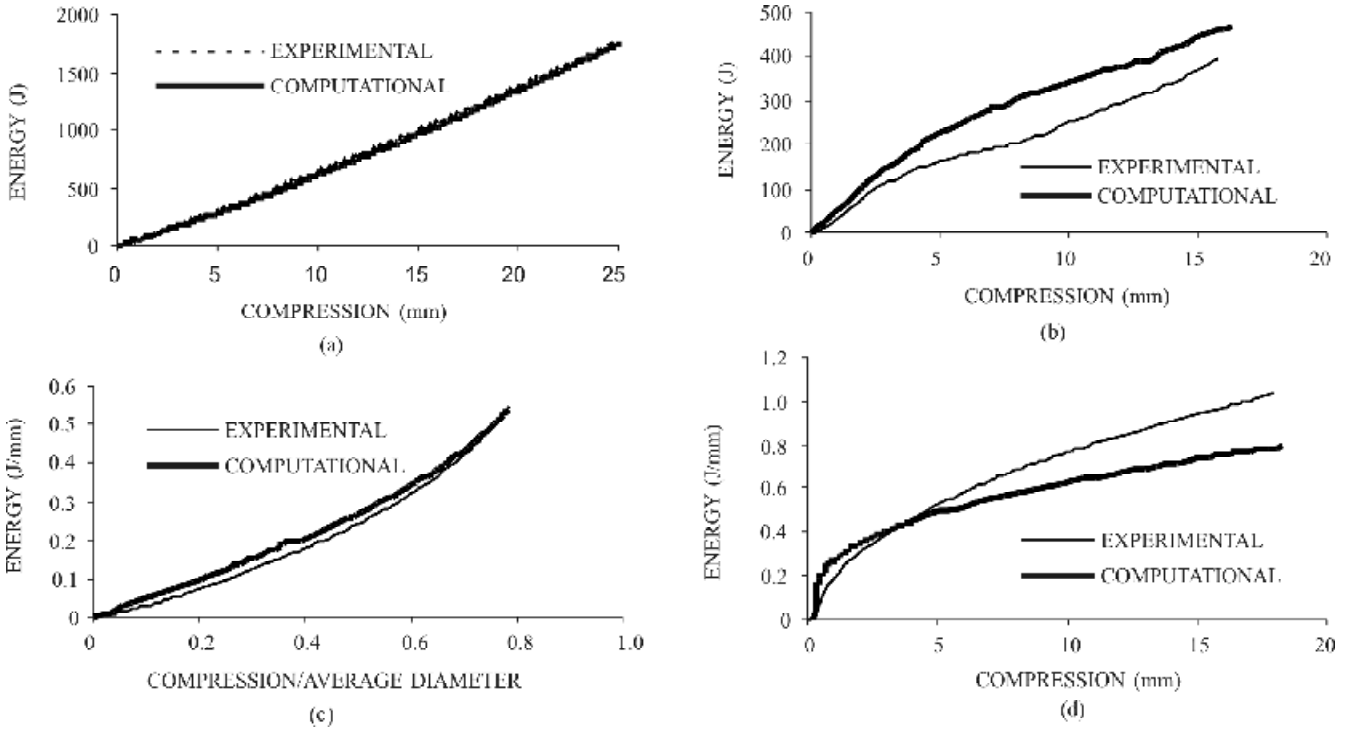

Figure 5. Comparison of experimental and computed energy-compression curves: (a) axisymmetric multiple barrelling of round tube subjected to axial load, (b) axisymmetric concertina mode of collapse of round tube subjected to axial load, (c) flattening of round tube subjected to lateral load, and (d) flattening of rectangular and square tubes subjected to lateral load.

3.1.1 Axisymmetric Multiple Barrelling of Round Tube Subjected to Axial Load

Figure 6(a) depicts the variation of equivalent strain (Eb) at two stages of compression process. The higher values of Eb occur at those points, which are also the place of largest change in curvature during the whole compression process. The contours appear to be co-centric about these points. The highest value of equivalent strain (Eb) is 2.59. It can be observed that at any horizontal section of the tube, the values of the Eb at different points are not equal. Moreover, the values of the Eb on those locations where the lowest curvature

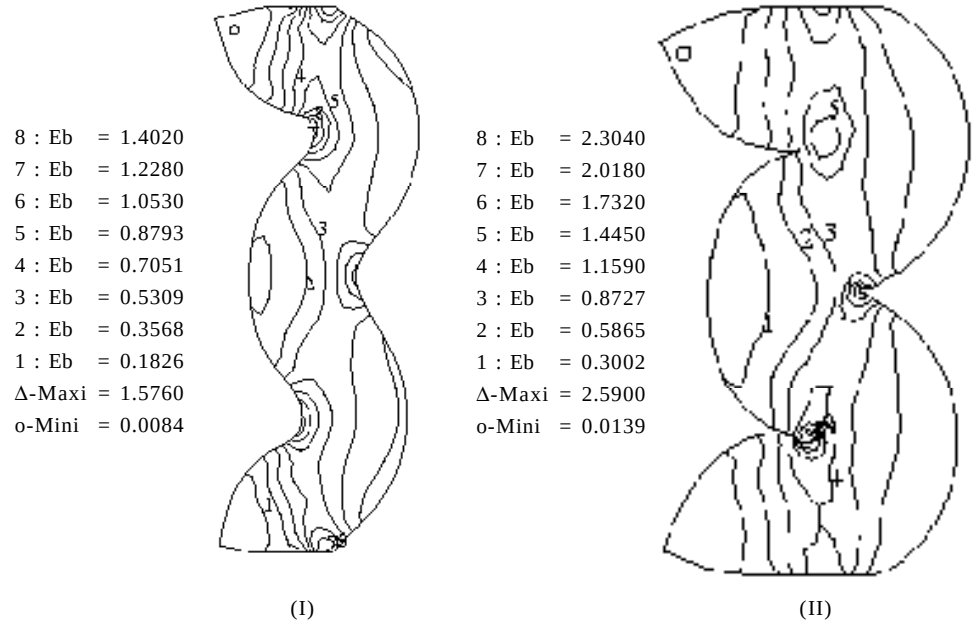

(a)

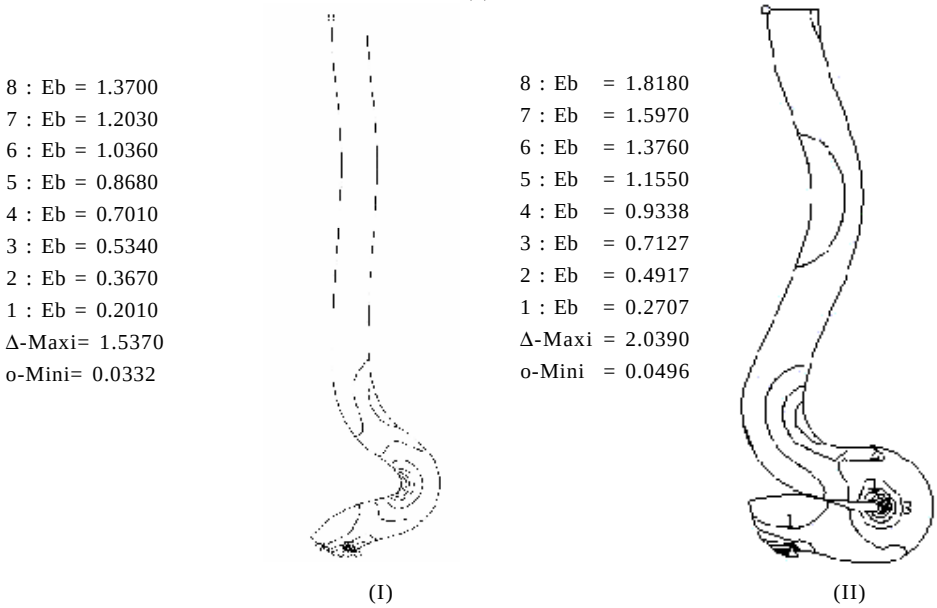

(b)

Figure 6[(a)-(b). Variations of predicted contours of equivalent strain at two stages in: (a) axisymmetric multiple barrelling of round tube subjected to axial load and (b) axisymmetric concertina mode of collapse of round tube subjected to axial load.

change occurs are almost the same. After seeing the variations of Eb, it is clear that the tube undergoes axial compression and bending. After observing the load-compression curve and the distribution of Eb, it is also clear that the major deformation occurs due to direct axial compression. Further more, it can also be concluded that during the compression process, the axisymmetric multiple-barrelling mode of collapse generate due to continuous deformation of the whole tube in axial compression with bending.

3.1.2 Axisymmetric Concertina Mode of Collapse of Round Tube Subjected to Axial Load

The variations of Eb is shown in Fig. 6(b) at the two stages of compression. It is clear from this figure that higher values of the Eb occur at two places. First is the area, which remains in contact with the top platen throughout the compression process, so that crushing of the material occurs in this area. The maximum value of Eb in this

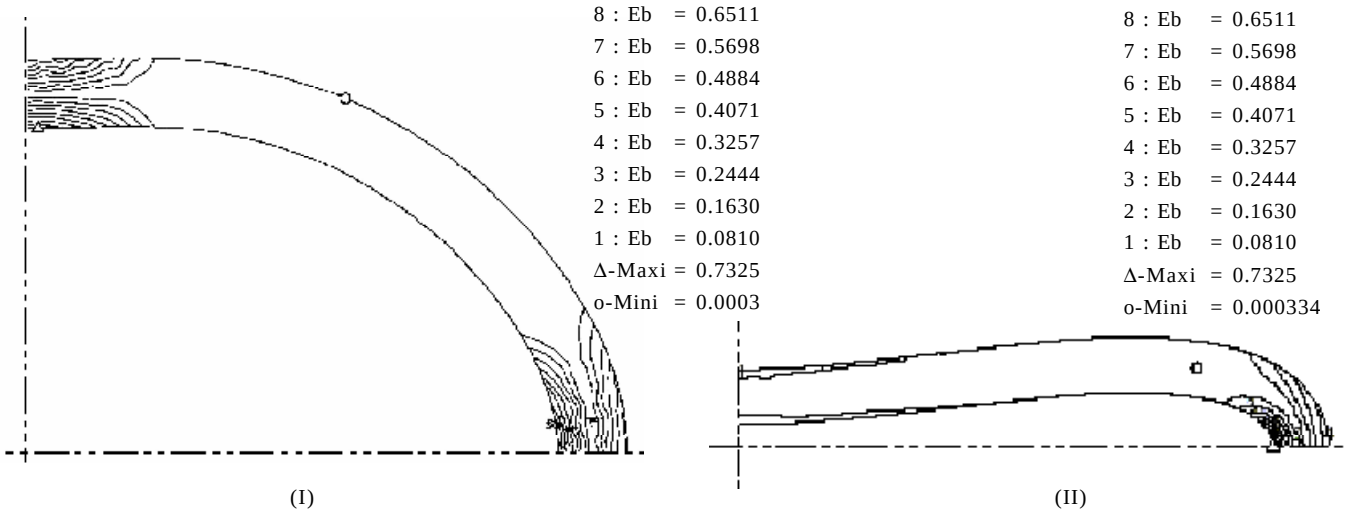

(c)

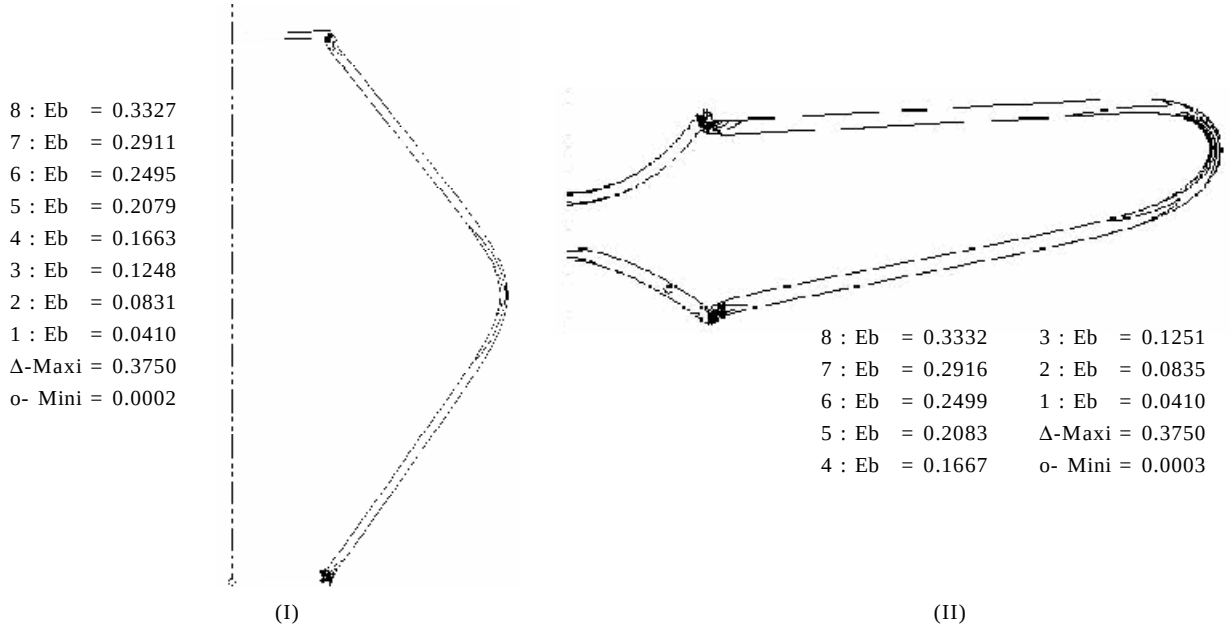

(d)

Figure 6[(c)-(d)]. Variations of predicted contours of equivalent strain at two stages in: (c) flattening of round tube subjected to lateral load and (d) flattening of rectangular and square tubes subjected to lateral load.

area is approx. 2. Second place, where the higher value contours of Eb occur, is the area, where the first plastic hinge forms which is also the seat of largest curvature change [Fig. 7(a)]. The deformations mainly concentrate in this region throughout the compression process. So the maximum value of Eb in this area is approx. 1.82. It can be seen that the concertina mode of collapse develops due to the complete formation of one plastic hinge [designated as first hinge in Fig. 7(a)].

3.1.3 Flattening of Round Tube Subjected to Lateral Load

The variations of Eb at the two stages of compression is shown in Fig. 6(c). It is clear from this figure that in the initial stage of compression, the major deformation occurs in the region around the vertical axis of symmetry of the tube. But later on, most of the deformation in tube takes place in the region which is on the horizontal axis of symmetry. The maximum value of equivalent strain in the zone, which falls on the vertical axis of symmetry, is only 0.155, whereas it is as high as 0.9005 in that zone which falls on the horizontal axis of symmetry. The Eb in the remaining portion of the tube is relatively very small throughout the compression process. Flattening of round tube due to lateral load occurs due to the formation of four plastic hinges at the intersection of horizontal and vertical axes of symmetry with the tube section. First set of two plastic hinges develops at the vertical axis of symmetry, which is the region of initial tube platen contact [Fig. 7(b)]. The second set of the two plastic hinges forms at the intersection of horizontal axis of symmetry and the tube [Fig. 7(b)].

3.1.4 Flattening of Rectangular and Square Tubes Subjected to Lateral Load

Figure 6(d) depicts the variations of Eb in rectangular tube at the two prominent stages of compression. It is clear from this figure that in the initial stage of compression, most of the deformation occurs at the two ends of the vertical wall of the tube. Hence, large strain develops in this region and ultimately plastic hinges form. On the other hand, during the remaining compression process, the deformation is predominant in the middle of the vertical wall of the tube. The highest value of Eb at the two ends of the vertical wall of the tube is 0.375, while at the middle of the wall, it is predicted to be 0.33. Flattening of rectangular

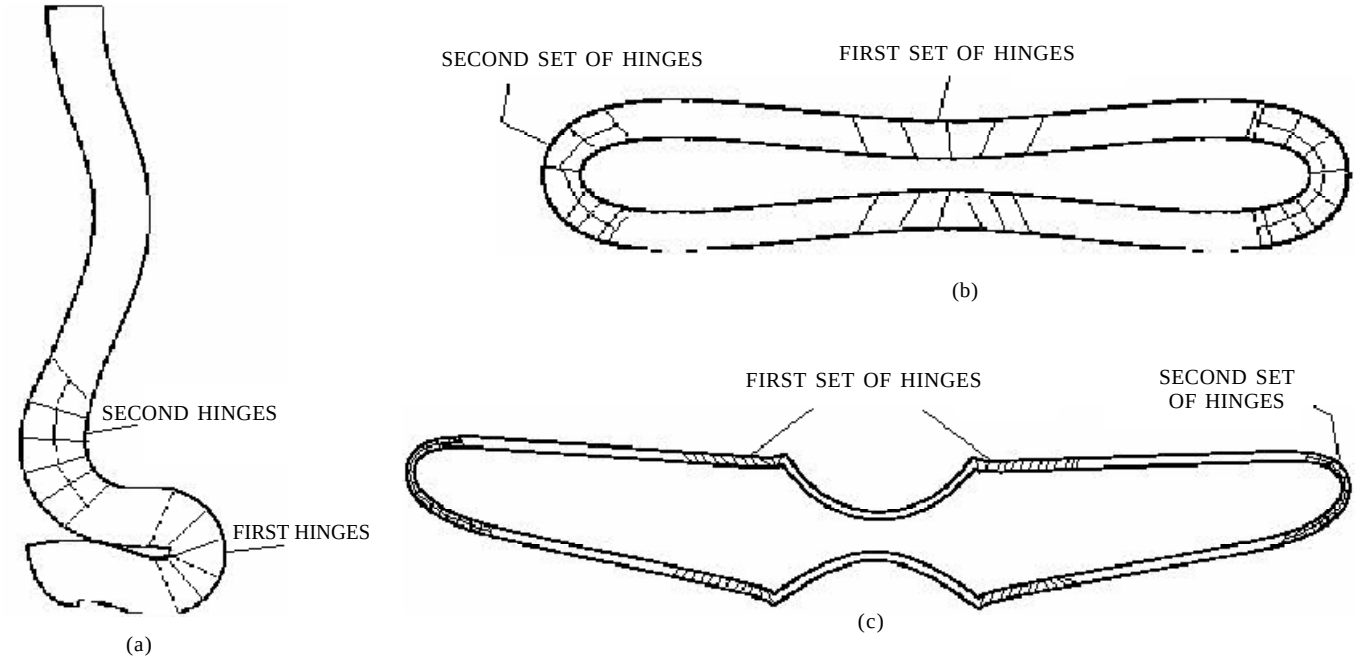

Figure 7. Development of hinges in: (a) axisymmetric concertina mode of collapse, (b) flattening of round tube, and (c) flattening of rectangular and square tubes.

Table 1(b). Dimensions of rectangular and square tubes subjected to lateral compression

Specimen	Width	Height	Thickness (mm)			Material properties		
	(mm)	(mm)	Vertical	Top	Bottom	K_0 (MPa)	*a*	*m*
AS3838	38.00	38.00	1.50	1.48	1.60	115.12	3.75	0.022
AS26262	25.44	25.44	2.18	1.74	2.20	108.50	4.16	0.028
AR5025	49.50	24.50	0.96	0.80	0.96	105.20	3.89	0.025
AS26263	25.36	25.36	2.20	2.34	2.34	108.50	4.11	0.029
AS26261	24.08	24.08	0.94	0.72	1.12	105.50	4.17	0.028
AR37251	35.68	24.00	0.72	0.76	0.72	107.50	4.15	0.029
AR2436	24.00	35.68	0.74	0.64	0.78	107.50	4.15	0.029
AR25372	24.86	36.38	1.60	1.58	1.74	109.50	4.05	0.028
AR2675	25.46	75.00	0.90	0.88	1.00	109.50	4.17	0.028
AR7526	75.00	25.46	0.95	0.90	0.88	109.50	4.17	0.028

and square tubes subjected to lateral load occurs due to the formation of six plastic hinges in two sets. First set of four plastic hinges forms at the two ends of the two vertical sides of the tube, while second set of two plastic hinges develops at the middle of the vertical sides of the tube [Fig. 7(c)].

4. CONCLUSIONS

The study presents extensive experimental and computational results on axial and lateral compression tests of metallic hollow tubes. Aluminium tubes were subjected to axial and lateral compression between the two rigid platens in an Instron machine. Load-compression curves and deformed shapes of the specimens at different stages of compression were recorded.

A finite element computational model for different compression processes is presented and an FEM analysis of compression process was carried out using FORGE2 code by considering the material as rigid-visco-plastic. Results thus obtained for load-compression curves and deformed shapes compare very well with the experiments. Further, these models can be employed to predict the mechanics of deformation of shells under different loading conditions.

REFERENCES

1. Jones, N. & Wierzbicki, T. Structural crashworthiness. Butterworth & Co, 1983.

2. Wierzbicki, T. & Jones, N. Structural failure. John Wiley & Sons, 1988.

3. Jones, N. & Wierzbicki, T. Structural crashworthiness. Elsevier Applied Science, 1983.

4. Gupta, N.K. Plasticity and impact mechanics. Wiley Eastern Ltd, New Delhi, 1993.

5. Gupta, N.K. Plasticity and impact mechanics. NewAge International (P) Ltd, New Delhi, 1996.

6. Ezra, Arthur A. & Fay, R.J. An assesment of energy-absorbing devices for prospective use in aircraft impact situations. *In* Dynamic response of structures,edited by G. Hormone, and N. Perron. Proceedings of a symposium held at Stanford University, California, 28-29 June 1972. pp. 225-46.

7. Johnson, W. & Reid, S.R. Metallic energy dissipating systems. *Appl. Mech. Rev.,* 1978, **31**, 277-88.

8. Andrews, K.R.F.; England, G.L. & Ghani, E. Classification of the axial collapse of cylindrical

tubes under quasi-static loading. *Int. J. Mech. Sci*., 1983, **25**, 687-96.

9. Alexander, J.M. An approximate analysis of the collapse of thin cylindrical shells under axial loading. *Q. J. Mech. Appl. Math.,* 1960, **13**, 1-9.

10. Abramowicz, W. & Jones, N. Dynamic axial crushing of circular tubes. *Int. J. Impact Engg*., 1984, **2**, 263-81.

11. Grzebeita, R.H. An alternate method for determining the behaviour of round stocky tubes subjected to an axial crush load. *Thin-walled Struct.,* 1990, **9**, 61-89.

12. Wierzbicki, T.; Bhat, T.; Abramowicz, W. & Brodikin, D. Alexander revisited - A two folding elements model of progressive crushing of tubes. *Int. J. Solids Struct*., 1992, **29**(24), 3269-288.

13. Gupta, N. K. & Velmurugan, R. Consideration of internal folding and non-symmetric fold formation axisymmetric axial collapse round tubes. *Int. J. Solids Struct.*, 1997, **34**, 2611-630.

14. Mutchler, L.D. Energy absorption of aluminium tubing. *J. Appl. Mech.*, 1960, **27**, 740-43.

15. De Runtz, J.A. & Hodge, P.G. Crushing of a tube between rigid plates. *J. Appl. Mech.*, 1963, **30**, 391-95.

16. Burton, R.H. & Craig, J.M. An investigation into the energy-absorbing properties of metal tubes loaded in the transverse direction. BSc (Engg) Report, University of Bristol, England, 1963.

17. Redwood, R.G. Discussion of crushing of a tube between rigid plates. *J. Appl. Mech.*, 1964, **31**, 357-58.

18. Reid, S.R. & Reddy, T.Y. Effect of strain hardening on the lateral compression of tubes between rigid plates. *Int. J. Solids Struct*., 1978, **14**, 213-25.

19. Reddy, T.Y. & Reid, S.R. Phenomena associated with their crushing of metal tubes between rigid plates. *Int. J. Solids Struct.,* 1980, **16**, 545-62.

20. Kecman. Bending collapse of rectangular and square section tubes. *Int. J. Mech. Sci.*, 1983, **25**(9-10), 623-36.

21. Sinha, D.K. & Chitkara, N.R. Determination of plastic collapse loads of rectangular tubes. *Acta Mechanica*, 1984, **51**, 199-215.

22. Gupta, N.K. & Khullar, A. Collapse load analysis of square and rectangular tubes subjected to transverse in plane loading. *Thin-walled Struct.*, 1995, **21**, 345-58.

23. Khullar, A. Transverse collapse of square and rectangular tubes and their layers. IIT Delhi, 1993. PhD Thesis.

24. Ray, P. Lateral collapse of empty and filled square tubes. IIT Delhi, New Delhi, 1995. PhD Thesis.

25. Horton, W.H.; Bailey, S.C. & Edward, A.M. Non-symmetric buckle pattern in progressing plastic buckling. *Experimental Mechanics*, 1966, 433-44.

26. Gupta, P.K. An investigation into large deformation behaviour of metallic tubes. IIT Delhi, New Delhi, 2000. PhD Thesis.

27. Bathe, K. J.; Walczak, J.; Guillermin, O.; Bouzinov, P.A. & Chen, H.Y. Advances in crush analysis. *Computers and Structures*, 1999, **72**, 31-47.

28. Mikkelsen, L.P. A numerical axi-symmetric collapse analysis of visco-plastic cylindrical shells under axial compression. *Int. J. Solids Struct.*, 1999, **36**, 643-68.

29. FORGE2. Finite element analysis code for metal-forming problems, Version 2.5, cemef, sofia Antipolis, France, 1992.

30. Hoff, N.J. Approximate analysis of structures in presence of moderately large creep deformations. *Q. J. Appl. Math*, 1954, **12**.

Contributors

Dr P.K. Gupta has been working at the Indian Institute of Technology (IIT) Roorkee. His areas of research are: Structural mechanics, finite element analysis, parallel computing and large deformations. He has vast experience in consultancy and teaching at undergraduate and postgraduate levels. He has edited one conference proceedings and published 35 research papers in different international and national journals and conferences. He has guided one PhD and six masters' theses. He is actively engaged in research and consultancy projects.

Prof N.K. Gupta is internationally well-recognised for his researches in the area of large deformations of metals and composites at low, medium, and high rates of loading. He has published his research work extensively in national and international journals, guided researches at PhD and MTech levels, and undertaken national and international research and consultancy projects. He has visited many countries in different capacities. He is recipient of *Erskine* (New Zealand) *Award* in 1995 and *Alexander von Humboldt* (Germany) *Award* in 1998. Prof Gupta was conferred with *Padma Shri* from the President of India in 1991.

Prof G.S. Sekhon has worked in different capacities at IIT Delhi, New Delhi, starting from Assistant Professor to Professor and Head of the Dept. He headed the department during 1996-99. His areas of specialisation include computational plasticity and finite element applications. He has served as Chairman of the Departmental Research Committee, and member of the Board of Postgraduate Studies of IIT Delhi and other universities also. He has published nearly 150 papers in journals and conference proceedings in the areas of finite element simulations, analysis of large deformation of metals, economics of manufacturing and cardio-vascular flows. He has written three books and edited eight conference proceedings. He has supervised 18 PhD theses.